

## INFLUENCE OF THE ULTRASONIC VIBRATION ON CHEMICAL BATH DEPOSITION OF ZnS THIN FILMS

QI LIU and GUOBING MAO  
*Mechanical Engineering Department  
Anhui University of Technology and Science  
Anhui Wuhu, 241000, China*

Received 8 July 2009

Chemical bath deposition (CBD) and ultrasonic chemical bath deposition (US-CBD) of ZnS thin films from  $\text{NH}_4\text{OH}/\text{SC}(\text{NH}_2)_2/\text{ZnSO}_4$  solutions have been studied. The influence of the ultrasonic vibration on properties of ZnS thin films has been investigated. The growth rate, structure, and properties of ZnS thin film deposited by different CBD techniques were studied using X-ray diffractometer (XRD), scanning electron microscopy (SEM), and atomic force microscope (AFM). The results show that the growth rate of US-CBD is slower than that of CBD. The XRD analysis of as-deposited ZnS films shows that the films are both cubic ZnS structure and the crystallinity of US-CBD ZnS film is higher than that of CBD ZnS film. SEM studies indicate that adhesion particles on the US-CBD ZnS surface are fewer than that on the CBD ZnS surface. Moreover, the film prepared by US-CBD is homogeneous and with high compactness. The rms roughness ( $R_{\text{rms}}$ ) value of CBD ZnS film is higher than that of US-CBD. Transmission measurement shows that the optical transmittance of US-CBD ZnS is higher than that of CBD ZnS, and the optical transmittance is above 90% when the wavelength is over 470 nm. The band gap ( $E_g$ ) values of the films deposited by CBD and US-CBD are 3.50 and 3.67 eV, respectively.

*Keywords:* Chemical bath deposition (CBD); ultrasonic chemical bath deposition (US-CBD); ultrasonic vibration; ZnS thin films.

### 1. Introduction

The conventional  $\text{CuIn}_x\text{Ga}_{1-x}\text{Se}_2$  (CIGS) thin film solar cells were typically fabricated using a cadmium sulfide (CdS) buffer layer.<sup>1</sup> The losses introduced by the CdS layer in the UV range will limit the level of the optimal performances of the cells. The higher short-circuit current ( $J_{\text{sc}}$ ) can be achieved by replacing CdS with other appropriate wider bandgap buffer materials. Moreover, the use of cadmium is undesirable from the viewpoint of environmental safety. One highly competitive alternative for CdS thin film is ZnS thin film.<sup>2</sup> It has a wider energy bandgap than CdS, which results in the transmission of more high-energy photons to the junction.

A low-cost approach for deposition of ZnS film on semiconductor or glass substrate is the chemical bath deposition (CBD) technique.<sup>3</sup> It is confirmed as a simple and promising technique to obtain device quality films. It is a low temperature, low cost, and scalable technique, which has been used in the fabrication of CIGS solar cells having 18.6% efficiency.<sup>4</sup>

In CBD, deposition of metal chalcogenide semiconducting thin films is done by maintaining the substrate in contact with the solution of chemical bath containing the metal and chalcogen ions. The film formation on substrate takes place when ionic product exceeds solubility product. There are two competitive processes in it, one is the heterogeneous

process of the solid film deposited on the substrate and the other is the homogeneous process of precipitation in the reaction bath.<sup>5,6</sup> The two processes compete with each other, which will influence the adhesive property between film and substrate. The mechanism for the heterogeneous process can be described as follows<sup>7,8</sup>:

- (1) “Ion by Ion” mechanism, adsorption of metal ion complex at the surface of substrates first, and then adsorption of thiourea to form metastable complex, formation of metal chalcogenide thin films by the metastable complex decomposition finally.
- (2) “Cluster by Cluster” mechanism leads to powdery and nonadherent films.
- (3) Mixed mechanism.

These three mechanisms are shown in Fig. 1. Generally, the film deposited by “Ion by Ion” mechanism is compact and smooth. But the other two mechanisms always coexist and couple with homogeneously in solution. These results are unnecessary precipitation on substrate and hamper the uniformity of the deposited film. The homogeneous process may be suppressed by using conditions for the formation of ZnS at low rates, such as low concentration of zinc salt and  $(\text{NH}_2)_2\text{CS}$ , high concentrations of  $\text{NH}_3$  and  $\text{NH}_4\text{Cl}$ , low temperature, etc. In order to reduce “Cluster by Cluster” mechanism, agitations can be used in CBD. There are two kinds of agitations commonly used in CBD. One is magnetic agitation, and the other is mechanical agitation.<sup>9,10</sup> Although the rate of agitation is high, there still exists some particles on the film which will reduce the crystallinity of the film and deteriorate adhesive property between film and substrate.

Ultrasonic vibration was applied in the CBD of ZnS thin films in this paper. It has been reported by Jun Young Choe *et al.*<sup>11</sup> that transparent and uniform CdS thin films can be obtained by CBD

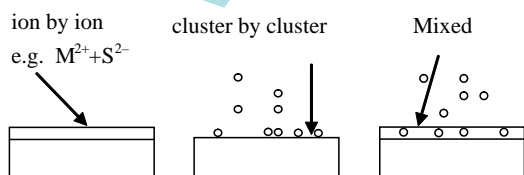


Fig. 1. Different mechanisms of deposited film.

technique under the catalytic activity of the ultrasonic vibration. Akira Ichiboshi *et al.*<sup>12</sup> improved the efficiency of CIGS devices through the use of ultrasonic vibration during the deposition of the  $\text{Zn}(\text{O},\text{OH})$  buffer layers. The fill factor (FF) and the diode quality factor of their CIGS devices are improved significantly. Little research has been conducted on the effects of ultrasonic vibration on properties of ZnS thin films.

The aim of this study is to investigate the influence of ultrasonic vibration on the ZnS thin film deposition by CBD through observing the changes in structural and morphological properties of ZnS films. In this paper, we name the CBD with mechanical agitation as CBD process, and the deposition with ultrasonic vibration as US-CBD process for convenience of expression.

## 2. Experimental

The depositions were carried out on commercial glasses. These were cleaned with detergent in an ultrasonic cleaner at  $70^\circ\text{C}$  (30 min), and then with deionized water and finally dried with  $\text{N}_2$ .

The solutions were prepared using analytical-grade reagents ( $\text{ZnSO}_4$ , thiourea, 25% ammonia). CBD ZnS thin films were chemically grown on glasses using a  $\text{ZnSO}_4$  (0.010–0.100 M), ammonia (0.07–0.37 M), thiourea (0.8–4 M) aqueous solution at  $75^\circ\text{C}$ .

The deposition solution is taken in a glass container. When the temperature reached the deposition temperature, precleaned glass slides were introduced into the solution and kept immersed in the solution at a few millimeters depth from the surface of the solution. For US-CBD, the chemical bath container and the substrates are immersed into a commercial ultrasonic cleaner (40 kHz).

After the glass substrates were removed, they were washed in running tap water, rinsed in deionized water to remove soluble impurities, and then dried with  $\text{N}_2$ . To enable the optical absorption, the films grown on the back side were removed by cotton swabs dipped in concentrated HCl.

The film thickness was measured using an AMB-LOS XP-1 profilometer. The surface morphology of as-deposited ZnS films was studied using Hitachi S-4800 scanning electron microscope (SEM) and CSPM4000 atomic force microscope (AFM). The

transmission measurements were made by SBP300 spectrum instrument in the wavelength range from 300 to 1100nm. X-ray diffraction patterns of the samples were recorded in Panalytical X'Pert Pro diffractometer with  $\text{CuK}\alpha$  radiation ( $\lambda = 1.5418 \text{ \AA}$ ) source over the diffraction angle  $2\theta$  between  $20^\circ$  and  $80^\circ$ .

### 3. Results and Discussion

The effect of ultrasound is the product of a phenomenon called cavitation. Billions of minute gas bubbles implode, causing shock waves that undermine dirt and blast it off a part's surface. Figure 2 shows the dependence of the ZnS thickness on the deposition time of CBD process and US-CBD process. As can be seen in this figure, the deposition rate of the ZnS layers by US-CBD process was slower than that of conventional CBD process. The decreased deposition rate in the initial stage of the

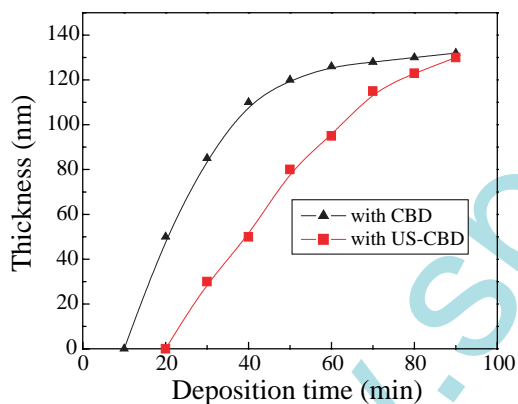


Fig. 2. The dependence of the ZnS thickness on the deposition time of CBD process.

US-CBD may be explained by ultrasonic vibration, which enhances the removal of secondary phase, and a removal of small particles from growing films.

Figure 3 shows the surface morphology of the ZnS thin films deposited by CBD and US-CBD process. The deposition time is 30 min and the temperature of bath is  $75^\circ\text{C}$ . In this figure, small colloidal particles are observed on the ZnS surface for the conventional CBD process. These particles could be amorphous. The film has a rough structure, the grain size is non-homogeneous. In contrast, almost no colloidal particles are present for the US-CBD process. The surface is smooth and the grain is homogeneous. The average size of grain is about 100 nm.

Figure 4 shows AFM images of ZnS thin films as shown in Fig. 3. Figure 4(a) corresponds to films prepared with CBD process. The rms roughness ( $R_{\text{rms}}$ ) value measured is 19.6 nm. Grains on films deposited with ultrasonic vibration seem to be more uniform and smooth, as can be observed in Fig. 4(b). The  $R_{\text{rms}}$  value is 6.88 nm. Ultrasonic vibration prevents the formation of colloidal particles, because of the high pressure and hot spots on surface.

The XRD pattern of the CBD and US-CBD ZnS film on glass substrate is shown in Fig. 5. The curve (a) of Fig. 5 is the XRD pattern of CBD ZnS film and curve (b) of Fig. 5 is XRD pattern of US-CBD ZnS film. From the curves, we can see that ZnS films show three diffraction peaks at  $29.6^\circ$ ,  $49.5^\circ$ , and  $58.7^\circ$  which are associated with the (111), (220), and (311) reflections of the cubic ZnS phase (JCPDS 79-0043). Comparing these two curves, we can see that the height of the peaks increase with ultrasonic vibration, which shows that the crystallinity of US-CBD ZnS thin film is superior to that of CBD ZnS film.

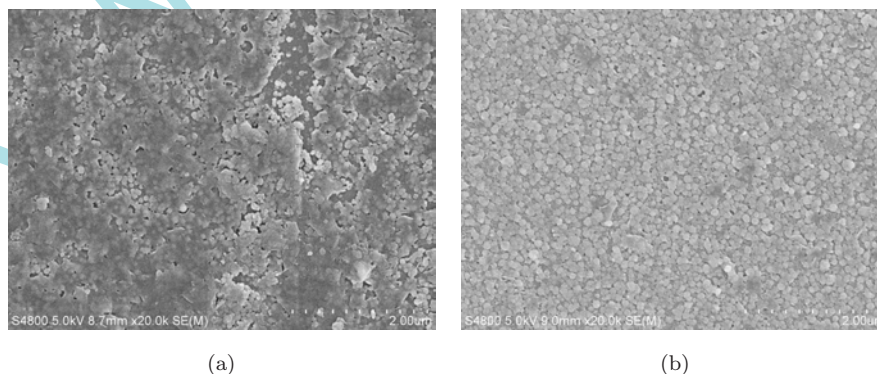


Fig. 3. SEM graphs of ZnS thin films deposited by: (a) CBD process, and (b) US-CBD process.

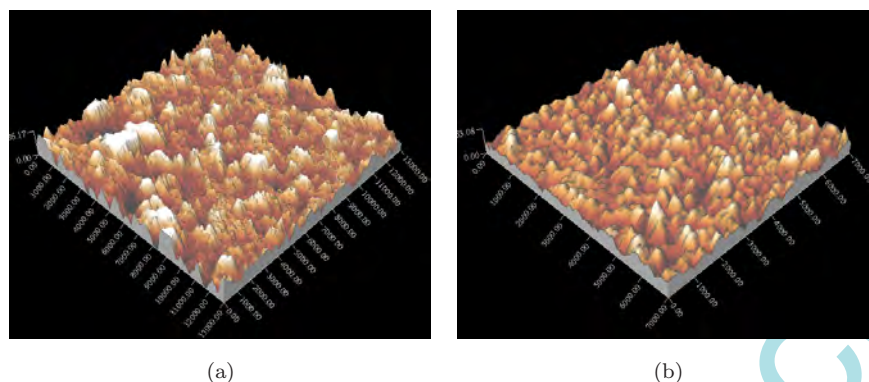


Fig. 4. AFM images of ZnS thin films deposited by: (a) CBD process, and (b) US-CBD process. Color online.

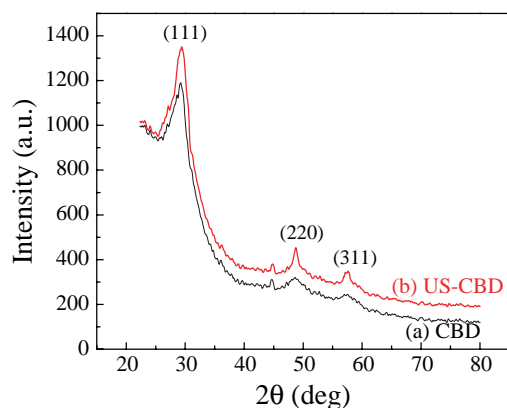


Fig. 5. X-ray diffraction patterns of ZnS thin films. Color online.

A fourth low intensity feature can be observed in the pattern at around  $2\theta = 45^\circ$ . These could be due to residual zinc sulfate (see JCPDF card 08-0491).

Figure 6 shows the optical transmission curves of 100 nm thick ZnS layers deposited by CBD and US-CBD processes. The absorption edge appears near the wavelength of 400 nm. The optical transmission of ZnS thin layer deposited with ultrasonic vibration is higher than that of conventional CBD process in all wavelength regions. The increased transmission is probably attributable to two aspects. First, the morphologies of two ZnS thin films are different. The rough surface morphology will reduce the transmission. The ultrasonic vibration removes the colloidal particles from the ZnS film. Second, the crystallinity of US-CBD ZnS thin film is superior to that of CBD ZnS film. The transmission of the US-CBD film is greater than 90% when the wavelength is above 400 nm. With US-CBD ZnS thin film as the buffer

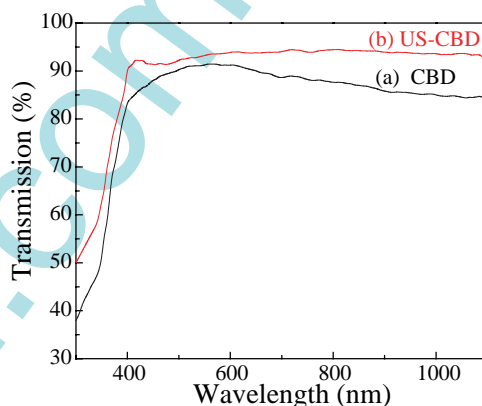


Fig. 6. Optical transmission spectra of ZnS thin films. Color online.

layer of CIGS solar cell will improve the short circuit current because more visible light can penetrate into the active region of solar cells. The shape of two curves is different in range 400–700 nm, this may be due to the difference in crystal structure and composition of the two thin films.

ZnS thin film is a direct bandgap semiconductor material, so the absorption coefficient,  $a$ , can be correlated to photon energy  $h\nu$ <sup>13</sup>:

$$(ah\nu)^2 = A(h\nu - E_g), \quad (1)$$

where “A” is a constant,  $h\nu = hc/\lambda$ ,  $h\nu$  is the photon energy,  $E_g$  is the value of the energy gap, and  $\lambda$  is the wavelength. The  $E_g$  of investigated ZnS thin films has been determined by extrapolating the linear  $ah\nu^2$  vs  $h\nu$  plot. The bandgaps of CBD and US-CBD ZnS thin films are found to be about 3.51 and 3.67 eV, respectively. As compared with the standard  $E_g$  value of ZnS thin film (3.8 eV), the two values are both lower. The reason may be that there

are impurities with low bandgap deposited into the ZnS film such as Zn(OH)<sub>2</sub>, ZnO. The bandgap value of US-CBD ZnS film is higher than that of CBD, which indicates that ultrasonic vibration decreases the impurity particles adhering to the films.

#### 4. Conclusion

Effects of ultrasonic vibration during CBD process of ZnS thin films have been investigated in this paper. The deposition rate of the ZnS layers by US-CBD process was slower than that of conventional CBD process. The surface of ZnS film is smoother and the grain is more uniform for the US-CBD process than that of CBD process. The rms roughness ( $R_{\text{rms}}$ ) value of CBD ZnS film is 19.6 nm and the  $R_{\text{rms}}$  value of US-CBD is 6.88 nm. The XRD analysis of ZnS films shows that the films are both cubic ZnS structure and the crystallinity of US-CBD ZnS film is higher than that of CBD ZnS film. The optical transmission of ZnS thin layer deposited with ultrasonic vibration is higher than that of conventional CBD process in all wavelength regions. The bandgaps of CBD and US-CBD ZnS thin films are found to be about 3.51 and 3.67 eV, the latter is more close to the standard  $E_g$  value of ZnS thin film.

#### References

1. M. A. Green, K. Emery and D. L. King, *Prog. Photovolt. Res. Appl.* **16** (2008) 61.
2. M. M. Islam, S. Ishizuka, A. Yamada, K. Sakurai, S. Niki, T. Sakurai and K. Akimoto, *Sol. Energy Mater. Sol. Cells* **93** (2009) 970.
3. L. Zhou, Y. Xue and J. Li, *J. Environmental Sci.* **21** (2009) S76.
4. R. N. Bhattacharya and K. Ramanathan, *Sol. Energy* **77** (2004) 679.
5. R. O. Borges and D. Linco, *J. Electrochem. Soc.* **140** (1993) 34.
6. M. A. Martinez, C. Guillen and J. Herrero, *Appl. Surf. Sci.* **136** (1998) 8.
7. P. O'Brien and J. McAleese, *J. Mater. Chem.* **18** (1998) 2309.
8. J. M. Dona and J. Herrero, *J. Electrochem Soc.* **144** (1997) 4081.
9. L. Qi, G. Mao and J. Ao, *Appl. Surf. Sci.* **254** (2008) 5711.
10. A. Goudarzi, G. M. Aval, R. Sahraei and H. Ahmadpoor, *Thin Solid Films* **516** (2008) 4953.
11. J. Y. Choe, K.-J. Kim, J.-B. Yoo and D. Kim, *Sol. Energy* **64** (1998) 41.
12. A. Ichiboshi, M. Hongo, T. Akamine, T. Dobashi and T. Nakada, *Sol. Energy Mater. Sol. Cells* **90** (2006) 3130.